

Finite superconducting square wire-network based on two-dimensional crystalline Mo_2C

Zhen Liu(刘震), Zi-Xuan Yang(杨子萱), Chuan Xu(徐川), Jia-Ji Zhao(赵嘉佶), Lu-Junyu Wang(王陆君瑜), Yun-Qi Fu(富云齐), Xue-Lei Liang(梁学磊), Hui-Ming Cheng(成会明), Wen-Cai Ren(任文才), Xiao-Song Wu(吴孝松), and Ning Kang(康宁)

Citation: Chin. Phys. B, 2022, 31 (**9**): 097404. DOI: 10.1088/1674-1056/ac67c7
Journal homepage: http://cpb.iphy.ac.cn; http://iopscience.iop.org/cpb

What follows is a list of articles you may be interested in

Induced current of high temperature superconducting loops by combination of exciting coil and thermal switch

Jia-Wen Wang(王佳雯), Yin-Shun Wang(王银顺), Hua Chai(柴华), Ling-Feng Zhu(祝凌峰), and Wei Pi(皮伟)
Chin. Phys. B, 2022, 31 (**3**): 037402. DOI: 10.1088/1674-1056/ac1f0a

Electronic properties and interfacial coupling in Pb islands on single-crystalline graphene

Jing-Peng Song(宋靖鹏) and Ang Li(李昂)
Chin. Phys. B, 2022, 31 (**3**): 037401. DOI: 10.1088/1674-1056/ac1b8e

Barrier or easy-flow channel: The role of grain boundary acting on vortex motion in type-II superconductors

Yu Liu(刘宇), Xiao-Fan Gou(苟晓凡), and Feng Xue(薛峰)
Chin. Phys. B, 2021, 30 (**9**): 097402. DOI: 10.1088/1674-1056/ac11ea

Dynamics of vortex-antivortex pair in a superconducting thin strip with narrow slits

An He(何安), Cun Xue(薛存), You-He Zhou(周又和)
Chin. Phys. B, 2017, 26 (**4**): 047403. DOI: 10.1088/1674-1056/26/4/047403

Field-dependent resistive transitions in $Yba_2Cu_3O_{7-\delta}$ thin films: Influence of the pseudogap on vortex dynamics

S H Naqib, R S Islam
Chin. Phys. B, 2015, 24 (**1**): 017402. DOI: 10.1088/1674-1056/24/1/017402

RAPID COMMUNICATION

Finite superconducting square wire-network based on two-dimensional crystalline Mo_2C

Zhen Liu(刘震)[1], Zi-Xuan Yang(杨子萱)[1], Chuan Xu(徐川)[2], Jia-Ji Zhao(赵嘉佶)[3], Lu-Junyu Wang(王陆君瑜)[3], Yun-Qi Fu(富云齐)[1], Xue-Lei Liang(梁学磊)[1], Hui-Ming Cheng(成会明)[2,4], Wen-Cai Ren(任文才)[2,4], Xiao-Song Wu(吴孝松)[3], and Ning Kang(康宁)[1,†]

[1] *Key Laboratory for the Physics and Chemistry of Nanodevices, School of Electronics and Center for Carbon-Based Electronics, Peking University, Beijing* 100871, *China*

[2] *Shenyang National Laboratory for Materials Science, Institute of Metal Research, Chinese Academy of Sciences, Shenyang* 110016, *China*

[3] *State Key Laboratory for Artificial Microstructure and Mesoscopic Physics, Frontiers Science Center for Nano-optoelectronics, Peking University, Beijing* 100871, *China*

[4] *School of Materials Science and Engineering, University of Science and Technology of China, Shenyang* 110016, *China*

(Received 8 March 2022; revised manuscript received 12 April 2022; accepted manuscript online 18 April 2022)

Superconducting wire-networks are paradigms to study Cooper pairing issues, vortex dynamics and arrangements. Recently, emergent low-dimensional crystalline superconductors were reported in the minimal-disorder limit, providing novel platforms to reveal vortices-related physics. Study on superconducting loops with high-crystallinity is thus currently demanded. Here, we report fabrication and transport measurement of finite square-network based on two-dimensional crystalline superconductor Mo_2C. We observe oscillations in the resistance as a function of the magnetic flux through the loops. Resistance dips at both matching field and fractional fillings are revealed. Temperature and current evolutions are carried out in magnetoresistance to study vortex dynamics. The amplitude of oscillation is enhanced due to the interaction between thermally activated vortices and the currents induced in the loops. The driving current reduces the effective activation energy for vortex, giving rise to stronger vortex interaction. Moreover, by the thermally activated vortex creep model, we derive the effective potential barrier for vortex dissipation, which shows well-defined correspondence with structures in magnetoresistance. Our work shows that low-dimensional crystalline superconducting network based on Mo_2C possesses pronounced potential in studying the modulation of vortex arrangements and dynamics, paving the way for further investigations on crystalline superconducting network with various configurations.

Keywords: superconducting wire-network, crystalline superconductor, vortex dynamics, low temperature transport

PACS: 74.78.–w, 74.81.Fa, 74.25.F–, 74.25.Ha **DOI:** 10.1088/1674-1056/ac67c7

1. Introduction

In a superconducting loop, due to the requirement of single-valued property in complex superconducting order parameter ψ, the phase φ changes by integral multiples of 2π, leading to flux quantization, with the flux quantum $\Phi_0 = h/2e$.[1,2] In the presence of magnetic field, the induced supercurrent in loop changes periodically, which tunes critical transition temperature T_c periodically, as revealed by oscillating magneto-resistance in Little–Parks experiments,[3–5] with oscillation period $H_0 = \Phi_0/S$, where S is the loop area. Subsequent studies extended phase-related characteristics into two-dimensional (2D) superconducting nanostructures.[6–23] This phase coherence in superconductors is an intrinsic property, providing a powerful tool for dealing with problems of superconductors under magnetic field, such as the pairing puzzles in insulating state,[6] anomalous metallic state[7] and magneto-resistance peak anomaly[8] in the superconducting to insulating transition (SIT), as well as pairing symmetry issues in unconventional superconductors.[24,25]

In terms of superconducting wire network, flux quantization is required at every single cell. What makes network different from single loop is that the arrangements of vortices are correlated, following the minimum-energy principle. Thus the vortex arrangement plays an essential role in determining T_c.[9–12] The value of magnetic field is described as filling factor $f = H/H_0$, where H is the applied field. When f equals an integer, due to the flux quantization, this corresponds to integral multiples filling of vortices in every unit cell of the network, accompanied by significant enhancement of T_c and large resistance dips. When f is a non-integer, nevertheless, at some specific fields, the arrangement pattern of vortex-lattice is energetically favored, leading to additional resistance dips at these fields, namely, fractional filling states.[9–12] Typically, the superconducting square-lattice network is a good candidate to experimentally study the arrangement of vortices.[13–17] For example, $f = 1/2$ represents an energetically favored checkerboard pattern, manifested by secondary dips of the magneto-resistance.[18–20]

†Corresponding author. E-mail: nkang@pku.edu.cn

© 2022 Chinese Physical Society and IOP Publishing Ltd

It is intriguing to study vortex dynamics in artificial superconducting nanostructures, which induce a modified potential for vortex motion. For example, interacting vortices confined in an asymmetric potential reveal ratchet effect and multiple drift reversals.[26] Signature of Weber blockade is observed in narrow superconducting nanowire with regular oscillation in magnetoresistance, corresponding to single vortex entry.[27] Besides, large oscillations of magnetoresistance in superconducting double network are caused by the interaction between thermally excited moving vortices and currents induced in the nanoloops.[21] However, quantitative description of the potential barrier for tunable vortex motion in superconducting network is still lacking.

Recently, the advance of technology for fabricating 2D crystalline superconducting materials with higher quality, lower disorder and less defects, is of great benefit to carry on phase-coherence related study.[28] It is highly demanded to develop loop structures and explore the phase-related physics and vortex physics in crystalline superconductors. Mo_2C crystal, grown by chemical vapor deposition (CVD) method, is an air-stable 2D high-quality crystalline superconductor with $T_c = 3$–4 K.[29] Recent study has shown that Mo_2C is an excellent platform to study the tuning of superconductivity and vortex related physics.[30–32] Therefore, it is tempting to study superconducting wire network structure in low-dimensional crystalline Mo_2C.

In this work, we fabricated finite superconducting square wire-network based on 2D crystalline Mo_2C by lithography and etching method, then carried out low-temperature electrical transport measurement. Magneto-resistance dips at both the integral and fractional filling factors are revealed. The amplitude of oscillating magneto-resistance versus temperature is larger than that predicated by the Little–Parks theory, due to the interaction between vortices and currents induced in the loop. Further increasing the driving current decreases the effective vortex excitation energy and gives birth to stronger vortex interaction. Moreover, effective potential barrier for vortex dissipation derived from vortex creep model oscillates and matches well with the periodicity in magneto-resistance. Our work demonstrates that Mo_2C crystalline superconducting wire-network provides a high-quality and promising platform to study vortex arrangements and dynamics.

2. Experiments

The as-grown 2D Mo_2C crystals were transferred onto SiO_2/Si substrates for device fabrication and electronic transport measurements. To avoid pinning effect at multi-domain boundaries, we selected rectangle and octagonal shaped samples with single domain.[30,31] Figure 1(a) shows the schematic of a standard four-terminal device of superconducting Mo_2C crystalline square network and the electrical measurement setup. The electrodes were first fabricated by the standard electron-beam lithography (EBL) followed by electron-beam evaporation (EVE) of bilayer-metal Ti/Au = 5/90 nm. Then we etched Mo_2C channel crystals via the mask of electron-beam resist defined by another EBL process. The etching was conducted in an inductive coupled plasma (ICP) enhanced reactive ion etching (RIE) equipment, whose recipes include 300 W RF power, 80 W ICP RF power, 50 sccm CF_4 as main etchant, 35 mTorr pressure and 30 s process time to ensure complete reaction of Mo_2C crystal. Figure 1(b) shows a scanning electronic microscopy (SEM) image from a part of an etched Mo_2C square-network sample Dev.01 with the inner loop size 400×400 nm^2 and the wire width 200 nm. The total number of unit square is $15\times20 = 300$. The low-temperature electrical transport measurements were conducted either in a physical property measurement system (PPMS) or a Dewar with variable temperature insert (VTI) equipment, cooling the sample down to 2 K with tunable magnetic field perpendicularly applied to the sample plane. An alternating current (AC) method using a lock-in amplifier at a low frequency of 17.777 Hz was employed with the driving current ranging from 10 nA to 100 μA.

3. Results and discussion

The inset of Fig. 1(c) shows resistance versus temperature with driving current 1 μA in Dev.01, from which superconducting transition can be observed. The critical transition temperature T_c is defined at which resistance equals $99\%R_n$, where R_n is the normal state resistance, yielding $T_c = 2.96$ K. The main panel of Fig. 1(c) shows the field dependence of the network resistance at 2.6 K, indicated by the green dot in the inset. We observed regular oscillations superposed on a parabolic background. This parabolic envelope stems from the contribution of the bulk of Mo_2C strips.[5,13] The oscillating period is $H_0 = 56.5$ Oe, corresponding to an effective loop area of $S = 0.366$ μm^2, which is equivalent to the length of side 605 nm. Due to the finite width $w = 200$ nm in Mo_2C strip, the equivalent length lies between the outer and inner boundaries for unit square. As shown by the white dashed box in Fig. 1(b), the actual effective area circles along the middle-line of the stripe, in reasonable agreement with the lattice parameter of the nano-patterned square network. Therefore, the periodic modulations pointed by black arrows are close to the Little–Parks effect, where each unit square is filled with integral multiple of vortices, leading to commensurate filling and forming an energetically stable lock-in state.[9]

Figure 1(d) is a magnification of the first oscillating period in Fig. 1(c), shaded in light canary. The abscissa is reduced to filling factor $f = H/H_0$ and the parabolic background has been subtracted. As indicated by the arrows, well-defined dips are observed at $f = 1/3$, $1/2$, $2/3$ and other fillings, in

addition to the fundamental dip at $f = \pm 1$. These dips at fractional fillings are associated with the commensurate arrangement of vortex-lattice with lower energy in the presence of underlying network.[33,34] Quantitatively, the phase boundaries are calculated in the spirit of mean-field theory by solving the linearized Ginzburg–Landau equation on the nodes.[9,10] This is analogous to the problem of an electron on a square lattice with unifrom magnetic field, whose energy spectrum is calculated in the tight-binding form by Hofstadter[35] and only the edge of the spectrum is related to superconducting-network problem. The factional fine structures in Fig. 1(d) are in agreement with the theory[9] and previous expriments,[13] indicating the effective interaction between vortex-lattice and underlying crystalline Mo_2C wire network.

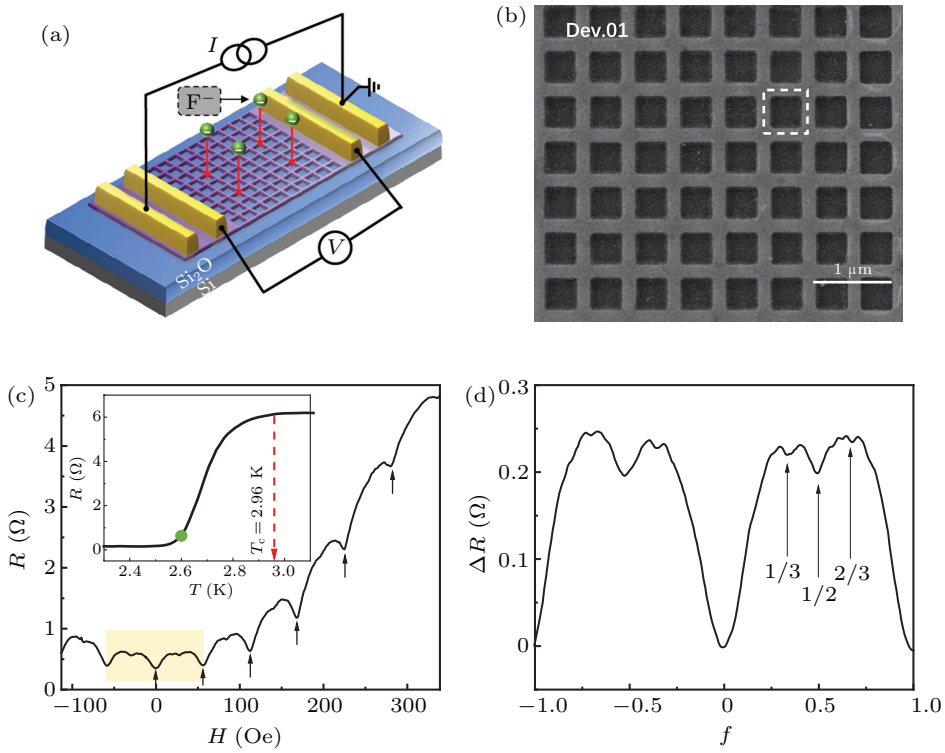


Fig. 1. (a) Schematic of four-terminal device and its electrical measurement for finite superconducting square wire-network based on 2D crystalline Mo_2C. The square network is fabricated by reactive ion etching with etchant CF_4. Green dots represent fluorinion excited by plasma. (b) SEM image of a part of network channel in Dev.01. The white dashed box indicates the effective loop area. (c) Magnetoresistance at 2.60 K. The arrows indicate the magnetic field values corresponding to integral number of filling factor $f = H/H_0$ per unit cell of the network. Inset shows resistance versus temperature with critical temperature $T_c = 2.96$ K. (d) Magnified view of the first period ($-H_0 \leqslant H \leqslant H_0$) of the critical line. In addition to the fundamental dips at $f = 0$ and ± 1, the secondary dips at $f = 1/3$, $1/2$, $2/3$ are indicated by the corresponding arrows.

Then, we conducted temperature evolution of magnetoresistance from 2.6 K to 2.78 K in Dev.01, as seen in Fig. 2(a). After subtracting the parabolic background, oscillating resistances ΔR versus filling factor f in the first period were plotted in Fig. 2(b). Mean variation of the oscillation resistance amplitude $\overline{\Delta R}$ was obtained by averaging over five periods of oscillation and shown as blue dots in Fig. 2(d). Notably, the $\overline{\Delta R}$ is non-monotonic with temperature, exhibiting the maximum amplitude around 2.65 K, which is closely related to vortex dynamics.[17] Initially, the activation energy of vortex decreases with increasing temperature, hence, the resistance amplitude climbs up at lower temperatures due to the rising effective vortex dissipation. However, this rise sees a turning point at 2.65 K, when stronger interaction between vortices decreases their mobility, giving rise to less effective dissipation, thus a drop of $\overline{\Delta R}$. In addition, temperature approaching T_c destroys superconducting phase coherence in network, further diminishing the $\overline{\Delta R}$.

This non-monotonic $\overline{\Delta R}$–T relation is reminiscent of the Little–Parks effect, in which the resistance oscillation amplitude is also non-monotonic in terms of $\Delta R = \Delta T_c(\mathrm{d}R/\mathrm{d}T)$.[3–5] The amplitude of oscillations in T_c is $\Delta T_c = 0.14 T_c(\xi_0/r)^2$,[1] where ξ_0 is the coherence length and r is the loop effective radius $r = (\Phi_0/\pi H_0)^{1/2} = 341.5$ nm. According to the Ginzburg–Landau coherence length for pure superconductor,[1] $\xi(T) = 0.74\xi_0(1 - T/T_c)^{-1/2}$, using typical value of $\xi(0) = 22$ nm at $T = 0$ K in Mo_2C[29] we estimated $\xi_0 \approx 30$ nm, which yields $\Delta T_c = 3.2$ mK. Then we can calculate oscillation amplitude ΔR with ΔT_c timing temperature derivative $\mathrm{d}R/\mathrm{d}T$ and the result is shown as black square symbols in Fig. 2(d). However, it can be seen that the amplitude by the Little–Parks theory is much samller than the measured ΔR.

Recent study focusing on the amplitude anomaly proposed a model that the enhancement of ΔR is due to the interaction between thermally excited moving vortices and

the oscillating persistent currents induced in the loops,[21,22] where the induced current is periodic stemming from the flux quantization,[2–5] with the derived ΔR as follows:

$$\Delta R = R_{\rm Loop}\frac{I_1(E_{\rm v}/2k_{\rm B}T)}{I_0(E_{\rm v}/2k_{\rm B}T)^3}\left[\frac{E_0}{2k_{\rm B}T}\right]^2, \quad (1)$$

where $R_{\rm Loop}$ is the effective resistance from the loop, I_1 and I_0 are respectively the first-order and zero-order modified Bessel functions of the first kind, $k_{\rm B}$ is the Boltzmann constant, $E_{\rm v}$ is the energy needed for creation of the vortex/antivortex in a ring, E_0 is associated with the interaction between a vortex or an antivortex and the current. Specifically, $E_{\rm v} = \Phi_0^2\ln[2w/\pi\xi(T)]/8\pi^2\Lambda(T)$, where w is the annulus width, $\xi(T) = 0.74\xi_0(1-T/T_{\rm c})^{-1/2}$ is the Ginzburg–Landau coherence length[1] and $\Lambda(T) = 2\lambda(T)^2/d$ is the Pearl penetration depth in a film of thickness d with the London penetration depth[1] $\lambda(T) = \lambda_0[1-(T/T_{\rm c})^2]^{-1/2}$, and $E_0 = \Phi_0^2\ln[(r+w/2)/(r-w/2)]/8\pi^2\Lambda(T)$.

In Dev.01, the film thickness is $d = 12$ nm measured by atomic force microscopy (AFM). Taking $r = 341.5$ nm into Eq. (1) to fit $\overline{\Delta R}$–T yields $\lambda_0 = 515$ nm, $\xi_0 = 30$ nm, $R_{\rm Loop} = 0.92\ \Omega$, $T_{\rm c} = 2.95$ K, $w = 190$ nm. The obtained parameters are physically reasonable. Note that the lithography and etching process may cause damage to the surface and sides and decreases the effective width. Nevertheless, the successful fitting in Fig. 2(d) indicates that the model[22] accounts well for our experiments and we conclude that the amplitude anomaly mainly stems from contribution of the vortex dynamics.

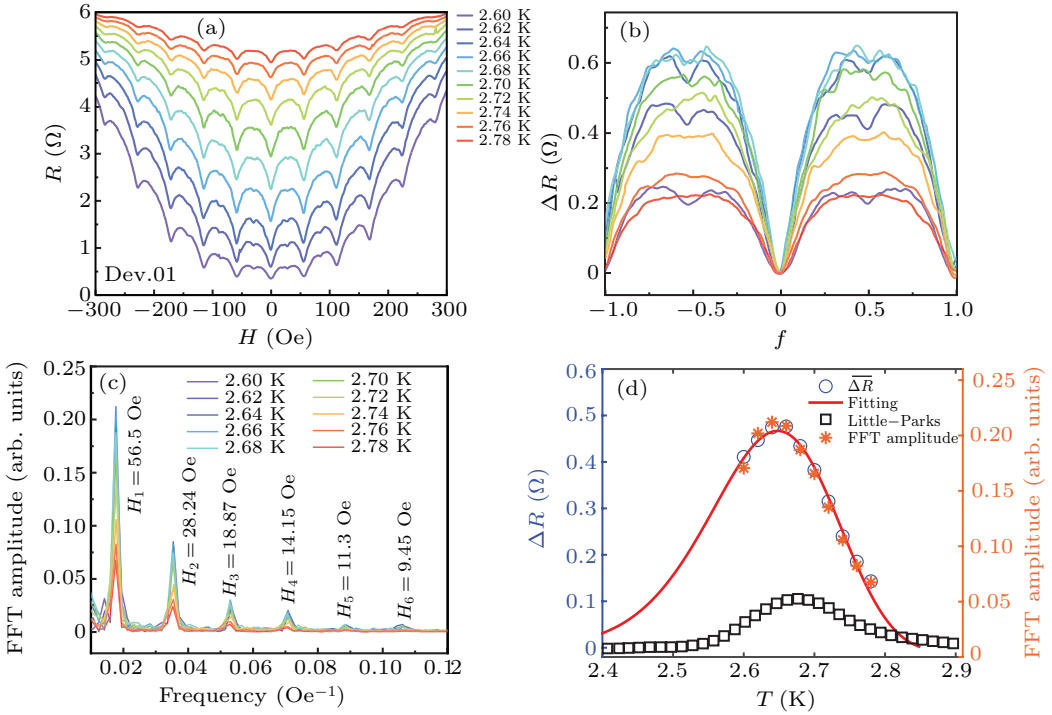


Fig. 2. (a) Resistance of the superconducting crystalline square-lattice as a function of magnetic field perpendicular to the sample plane at different temperatures from 2.6 K to 2.78 K. (b) Magnified view of the first period ($-H_0 \leqslant H \leqslant H_0$) of the critical line in (a) after subtracting a parabolic background. (c) FFT for ΔR–T in (b) from 2.6 K to 2.78 K. Amplitude peaks denoted by H_1, H_2, H_3, H_4, H_5 and H_6 correspond to oscillation periods of 56.5 Oe, 28.24 Oe, 18.87 Oe, 14.15 Oe, 11.3 Oe and 9.45 Oe, respectively, in line with the integral and fractional fillings in magnetoresistance. (d) Temperature dependence of the mean oscillation amplitude (blue circles) corresponds to y-axis on the left side. The red solid line is fitted with Eq. (1). The black squares show the resistance oscillations amplitude calculated for the Little–Parks effect. The orange snowflake symbols represent the amplitude of FFT for H_1 corresponding to the y-axis on the right side.

Apart from tuning the ΔR with temperature, as seen in Fig. 2(b), fine structures at fractional fillings gradually disappear with rising temperature. Nevertheless, resistance dips at $f = N$, where N is an integer, still survive at 2.78 K, indicating more stable vortex-arrangement in integral filling than that of fractional filling. This characteristic is obvious by performing fast Fourier transform (FFT) analysis in ΔR–H. Figure 2(c) depicts temperature evolution of FFT. Notably, multiple amplitude-peaks versus frequency are revealed, corresponding to $H_1 = 56.5$ Oe, $H_2 = 28.24$ Oe, $H_3 = 18.87$ Oe, $H_4 = 14.15$ Oe, $H_5 = 11.3$ Oe and $H_6 = 9.45$ Oe, as labeled in the figures. H_1 equals the H_0, the interval between adjacent dips of integral fillings in Figs. 1(c) and 2(a), thus H_1 corresponds to the period of magneto-resistance oscillation. The relation of these peaks follows $H_1 = 2H_2 = 3H_3 = 4H_4 = 5H_5 = 6H_6$. Hence, H_2 denotes period at $f = \frac{1}{2}+N$, and H_3, H_4 are related to structures at $f = \frac{1}{3}$ or $\frac{2}{3}+N$ and $f = \frac{1}{4}$ or $\frac{3}{4}+N$, respectively. H_5 is related to structures at integral multiple of $f = \frac{1}{5}$. H_6 could be the rational structures at $f = \frac{1}{6}$ or $\frac{5}{6}+N$, as well as the difference between structures at $f = \frac{1}{2}+N$ and $f = \frac{1}{3}$ or $\frac{2}{3}+N$. In addition, the amplitude of these peaks declines monotonically from H_1 to H_4, suggesting that vor-

tex arrangement at $f = \frac{1}{2} + N$ is the most stable type among the fractional fillings in terms of temperature, while less stable than that of $f = N$. The FFT amplitudes versus temperature from H_1 to H_4 follow the similar non-monotonically trend of variation, while the changes of FFT amplitude for H_5 and H_6 are too small to distinguish. We plot typical data of H_1 in Fig. 2(d), in good accord with the non-monotonic behavior of $\overline{\Delta R}$–T.

Since we have elucidated temperature evolution of vortex in the superconducting network, it worths noting that driving current can also tune the vortex dynamics effectively. Specially, we fixed the temperature near the largest resistance oscillation amplitude, denoted by the green dot in the cooling curve for Dev.02 in Fig. 3(a). The current evolution of magneto-resistance after subtracting parabolic background is seen in Fig. 3(b). Six periods are shown and the signal-to-noise ratio is relative poor in the lower current regimes. Nevertheless, FFT analysis reveals multiple peaks at H_1 and H_2, corresponding to $f = N$ and $f = \frac{1}{2} + N$, respectively, indicating effective interaction between vortex-lattice and underlying network. $\overline{\Delta R}$–I and FFT amplitude at H_1 are obtained in the same way above and plotted in Fig. 3(d), displaying monotonic decrease trend versus increasing current.

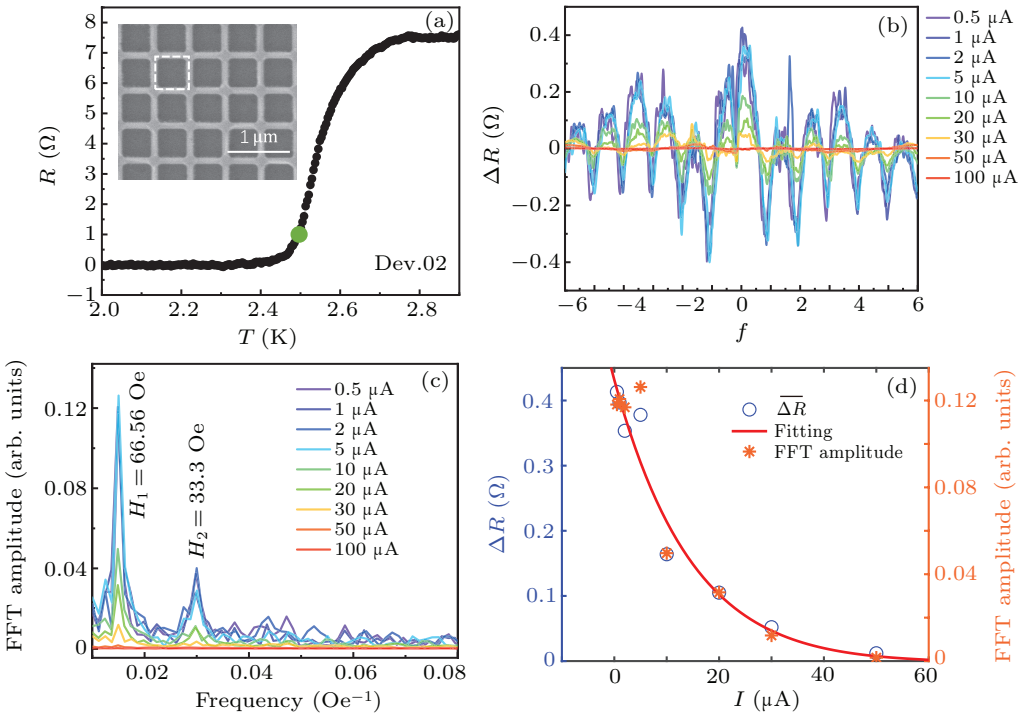


Fig. 3. (a) Resistance versus temperature with the driving current 0.1 μA for Dev.02. Inset: SEM image of a part of square-network channel. The white dashed box indicates the effective loop area. (b) Variation of resistance for the superconducting crystalline square-lattice as a function of magnetic field perpendicular to the sample plane with different driving currents from 0.5 μA to 100 μA. (c) FFT for ΔR–T in (b) from 0.5 μA to 100 μA. Amplitude peaks denoted by H_1 and H_2 correspond to oscillation periods of 66.56 Oe and 33.3 Oe, respectively, in line with the structures at $f = N$ and $\frac{1}{2} + N$ in magnetoresistance, where N is an integer. (d) Temperature dependence of the mean oscillation amplitude (blue circles) corresponds to y-axis on the left side. The red solid line is fitted based on a phenomenological model in the main text. The orange snowflake symbols represent the amplitude of FFT for H_1 corresponding to y-axis on the right side.

In the presence of field, thermally assisted creeping of vortices over pinning energy barrier contributes to the dissipation,[1,36,37] which can be described by an Arrhenius activation law

$$R = R_0 \exp\left(-\frac{U}{k_B T}\right), \tag{2}$$

where k_B is the Boltzmann constant, R_0 is the preexponential factor, and U is the flux pinning energy or activation energy for flux creep that depends on the strength of the applied magnetic field. It can be seen that the contribution to the resistance is closely related to the flux activation energy U.

Inspired by the thermally activated flux creep model, the influence of increasing the driving current should reduce the effective activation energy of vortex for dissipation, leading to enhanced density of dissipative-vortex. At the temperature point where ΔR is the largest, the vortices work in the most dissipative way. Further increasing the driving current creates excessive dissipative-vortices that interact with each other, leading to lower efficiency for dissipation, which accounts for the monotonic decrease of $\overline{\Delta R}$–I.

To quantitatively illustrate the $\overline{\Delta R}$–I relation, we defined effective activation energy of vortex creeping that contributes to the variation of resistance $U_{\rm eff}(I)$, which can be reduced by increasing currents, following phenomenologically as $U_{\rm eff}(I) = U_{\rm eff}[1 - (I/I_c)^{\alpha}]$, where I_c is the critical current and α is the fitting factor. Replacing $U_{\rm eff}(I)$ into Eq. (2),

we obtained the variation of resistance oscillation amplitude $\Delta R = R_0 \exp[U_{\rm eff}(I)/k_{\rm B}T_0]$, where $T_0 = 2.5$ K is the fixed temperature. We used this equation to fit $\overline{\Delta R}$–I in Fig. 3(d), which yields $U_{\rm eff}(I)/k_{\rm B}T_0 = 5.5$, $\alpha = 0.75$, $I_{\rm c} = 60$ μA. The phenomenologically fitting agrees well with the $\overline{\Delta R}$–I relation and thus illustrates that the driving current decreases the effective activation energy of vortex creeping.

In continues and uniform 2D superconducting films, activation energy for vortex creep is observed to decrease monotonically with the applied magnetic field.[38,39] In contrast, in superconducting films nanopatterned into a network of loops, this activation energy becomes oscillatory, due to the periodic potential barrier by the network combined with the interaction between moving vortices and currents induced in nanoloops,[21,22] as we have shown in Fig. 2(d). The equivalent effective potential barrier for vortex motion can be analyzed in terms of Eq. (2).

Hence, to obtain the relation between effective potential barrier and field strength, we carried out measurement of resistance versus temperature under a series of magnetic field strength, as seen in Fig. 4(a), with the driving current of 5 μA. The magnetic field gradually shifts R–T curves to lower temperature, with the critical field at about $20H_0$. In Fig. 4(b), we show an Arrhenius plot of the R–T with the same data in Fig. 4(a). The data exhibits clear thermal activation behavior just below $T_{\rm c}$, indicated by straight black dashed lines. We then can deduce the effective potential barrier from the linear fits to the activated region shown in Fig. 4(b), and the obtained $U/k_{\rm B}$ together with magneto-resistance are plotted in Fig. 4(c) with the same reduced abscissa f.

The $U/k_{\rm B}$–f shows periodical oscillation superposed on a downward trend with increasing f. Notably, this characteristic is inverse with that of magneto-resistance. When $f = N$, the vortex-lattice matches network well[9,10] and the lock-in of vortices is strongest as evidenced in Figs. 2 and 3. Besides, there is no induced current at $f = N$ and no interaction occurs between vortices and induced currents. Hence, the energy cost for dragging a vortex to be dissipative is the largest, which corresponds to the maximum of U at $f = N$. When $f = \frac{1}{2} + N$, the vortex-lattice forms checkerboard pattern.[18–20] This is the most energetically-stable arrangement among fractional fillings, as evidenced by Figs. 2(c) and 3(c), though, less stable than that of $f = N$. Therefore, the amplitude variation of $U/k_{\rm B}$ at $f = \frac{1}{2} + N$ should be larger than other fractional fillings in the same period and smaller than adjacent $f = N$. This characteristic is confirmed in the first period by $U/k_{\rm B}$ from $f = 0$ to $f = 1$, where at $f = \frac{1}{2}$ a peak appears. As a result, $U/k_{\rm B}$–f oscillates between adjacent $f = N$ and $f = \frac{1}{2} + N$, providing us with quantitative demonstration that the effective potential barrier for vortex dissipation oscillates periodically with the field strength in the presence of underlying network.

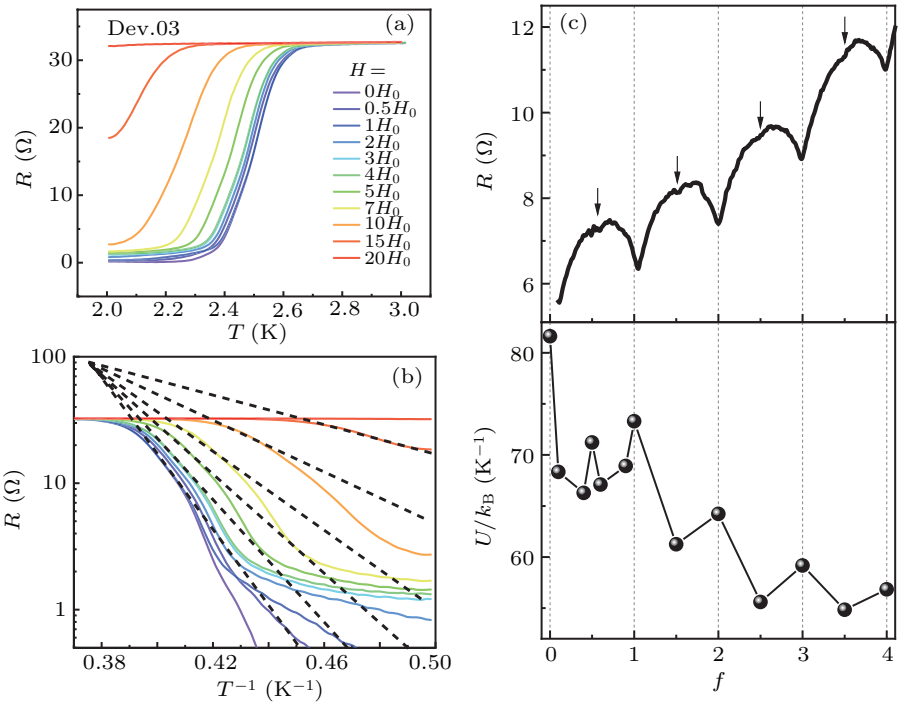


Fig. 4. (a) Superconducting resistive transition of crystalline square-lattice Dev.03 at a series of fixed perpendicular magnetic fields. H_0 is one integral oscillation period. (b) Arrhenius plot of the resistive transition in (a), indicating the thermally activated behavior. The black dashed lines are corresponding fitting curves using the collective flux creep model described by Eq. (2). (c) Magnetic field dependence of the activation energy $U/k_{\rm B}$ (lower panel), which is obtained from fitting in (b). The upper panel shows the typical magnetoresistance. Note that the $U/k_{\rm B}$ oscillates and matches well with the resistance structures.

4. Conclusion

To conclude, we have fabricated finite 2D superconducting square network based on crystalline Mo_2C and observed resistance dips at both integral and fractional filling factors. The enhanced amplitude of resistance oscillation is attributed to interaction between thermally activated vortices and currents induced in the loops. Increasing the driving current declines activation energy for vortex, which in turn, leads to stronger vortex interaction and lower vortex mobility. The effective potential barrier for vortex dissipation oscillates periodically, synchronously and inversely with magneto-resistance in terms of underlying network. Our work demonstrates that the finite crystalline superconducting network based on Mo_2C provides effective periodic potential barrier for vortex-lattice, and is a novel, clean and high-quality platform to study vortex arrangements and dynamics.

Acknowledgements

Project supported by the National Natural Science Foundation of China (Grant Nos. 11974026, 11774005, and 51802314), the National Key Research and Development Program of China (Grant No. 2017YFA0303304), Science Foundation of Jihua Laboratory (Grant No. 2021B0301030003-03), and the Strategic Priority Research Program of Chinese Academy of Sciences (Grant No. XDB30000000). Dr. C. Xu acknowledges the support of the Youth Innovation Promotion Association of Chinese Academy of Sciences.

References

[1] Tinkham M 2004 *Introduction to superconductivity* (Courier Corporation) pp. 127–130
[2] Deaver Jr B S and Fairbank W M 1961 *Phys. Rev. Lett.* **7** 43
[3] Little W and Parks R 1962 *Phys. Rev. Lett.* **9** 9
[4] Parks R and Little W 1964 *Phys. Rev.* **133** A97
[5] Groff R and Parks R 1968 *Phys. Rev.* **176** 567
[6] Stewart Jr M, Yin A, Xu J and Valles Jr J M 2007 *Science* **318** 1273
[7] Yang C, Liu Y, Wang Y, *et al*. 2019 *Science* **366** 1505
[8] Gurovich D, Tikhonov K S, Mahalu D and Shahar D 2015 *Phys. Rev. B* **91** 174505
[9] Kato M and Sato O 2013 *Supercond. Sci. Technol.* **26** 033001
[10] Rammal R, Lubensky T and Toulouse G 1983 *Phys. Rev. B* **27** 2820
[11] Lin Y L and Nori F 2002 *Phys. Rev. B* **65** 214504
[12] Chi C, Santhanam P and Blöchl 1992 *J. Low. Temp. phys.* **88** 163
[13] Pannetier B, Chaussy J, Rammal R and Villegier J 1984 *Phys. Rev. Lett.* **53** 1845
[14] Ling X, Lezec H, Higgins M, Tsai J, Fujita J, Numata H, Nakamura Y, Ochiai Y, Tang C, Chaikin P, *et al.* 1996 *Phys. Rev. Lett.* **76** 2928
[15] Yu F, Israeloff N, Goldman A and Bojko R 1992 *Phys. Rev. Lett.* **68** 2535
[16] Wilks C W, Bojko R and Chaikin P M 1991 *Phys. Rev. B* **43** 2727
[17] Van der Zant H, Webster M, Romijn J and Mooij J 1994 *Phys. Rev. B* **50** 340
[18] Behrooz A, Burns M, Levine D, Whitehead B and Chaikin P 1987 *Phys. Rev. B* **35** 8396
[19] Itzler M, Behrooz A, Wilks C, Bojko R and Chaikin P 1990 *Phys. Rev. B* **42** 8319
[20] Teitel S and Jayaprakash C 1983 *Phys. Rev. Lett* **51** 1999
[21] Sochnikov I, Shaulov A, Yeshurun Y, Logvenov G and Božović I 2010 *Nature Nanotech.* **5** 516
[22] Sochnikov I, Shaulov A, Yeshurun Y, Logvenov G and Božović I 2010 *Phys. Rev. B* **82** 094513
[23] Sochnikov I, Božović I, Shaulov A and Yeshurun Y 2011 *Phys. Rev. B* **84** 094530
[24] Juričić V, Herbut I F and Tešanović Z 2010 *Phys. Rev. Lett.* **100** 187006
[25] Berg E, Fradkin E and Kivelson S A 2009 *Nat. Phys.* **5** 830
[26] de Souza Silva C C, Van de Vondel J, Morelle M and Moshchalkov V V 2006 *Nature* **440** 651
[27] Morgan-Wall T, Leith B, Hartman N, Rahman A and Marković N 2015 *Phys. Rev. Lett.* **114** 077002
[28] Saito Y, Nojima T and Iwasa Y 2017 *Nat. Phys.* **2** 16094
[29] Xu C, Wang L, Liu Z, Chen L, Guo J, Kang N, Ma X L, Cheng H M and Ren W 2015 *Nat. Mater.* **14** 1135
[30] Liu Z, Xu C, Kang N, Wang L, Jiang Y, Du J, Liu Y, Ma X L, Cheng H M and Ren W 2016 *Nano Lett.* **16** 4243
[31] Liu Z, Wang C, Xu C, Hao M, Cheng H M, Ren W and Kang N 2019 *2D Mater.* **6** 021005
[32] Xu C, Liu Z, Zhang Z, Liu Z, Li J, Pan M, Kang N, Cheng H M and Ren W 2020 *Adv. Mater.* **32** 2002825
[33] Grest G S, Chaikin P M and Levine D 1988 *Phys. Rev. Lett.* **60** 1162
[34] Halsey T C 1985 *Phys. Rev. B* **31** 5728
[35] Hofstadter D R 1976 *Phys. Rev. B* **14** 2239
[36] FeigelMan M, Geshkenbein V, Larkin A and Vinokur V 1989 *Phys. Rev. B* **63** 2303
[37] Anderson P W and Kim Y 1964 *Phys. Rev. B* **36** 39
[38] Saito Y, Kasahara Y, Ye J, Iwasa Y and Nojima T 2015 *Science* **350** 409
[39] Tsen A, Hunt B, Kim Y, Yuan Z, Jia S, Cava R, Hone J, Kim P, Dean C and Pasupathy A 2016 *Nat. Phys.* **12** 208